Microgels for Efficient Protein Purification

Published in final edited form as:
Adv Mater. 2011 September 22; 23(36): H258–H262. doi:10.1002/adma.201101258.

Microgels for Efficient Protein Purification

Boaz Mizrahi, Dr.,
Children's Hospital Boston Division of Critical Care Medicine, Harvard Medical School, 300 Longwood Avenue. Bader 634 Boston, MA 02115, USA; Department of Chemical Engineering, Massachusetts Institute of Technology, Cambridge, MA 02139, USA

Silvia Irusta,
Institute of Nanoscience of Aragón, University of Zaragoza, Mariano Esquillor s/n, Zaragoza, 50018, Spain

Marshall McKenna,
Department of Chemical Engineering, Massachusetts Institute of Technology, Cambridge, MA 02139, USA

Cristina Stefanescu,
Children's Hospital Boston Division of Critical Care Medicine, Harvard Medical School, 300 Longwood Avenue. Bader 634 Boston, MA 02115, USA

Liron Yedidsion, Dr.,
Operations Research Center, Massachusetts Institute of Technology, Cambridge, MA 02139, USA

MyatNoeZin Myint,
Department of Chemical Engineering, Massachusetts Institute of Technology, Cambridge, MA 02139, USA

Robert Langer, Prof., and
Department of Chemical Engineering, Massachusetts Institute of Technology, Cambridge, MA 02139, USA

Daniel S. Kohane, Prof.
Children's Hospital Boston Division of Critical Care Medicine, Harvard Medical School, 300 Longwood Avenue. Bader 634 Boston, MA 02115, USA

Daniel S. Kohane: daniel.kohane@childrens.harvard.edu

Immobilized metal affinity chromatography (IMAC) is the most frequently used method for the separation and purification of histidine-tagged (His-tagged) proteins.[1] In this technique, the high affinity of metal ions, such as nickel or copper, to a tag sequence of the protein of interest creates strong, yet reversible binding.[2] A major limitation of current systems is their inefficiency in purifying many recombinant proteins, particularly when

Correspondence to: Daniel S. Kohane, daniel.kohane@childrens.harvard.edu.

Supporting Information: Supporting Information is available from the Wiley Online Library or from the author.

present in their native state or in low concentrations in the cell lysate.[3,4] Performance deficiencies are caused in part by the clogging or destruction of matrix micropores by undissolved salts and other compounds during particle synthesis,[5] limiting the surface area accessible for binding[6,7] (Figure S1 in the Supporting Information). Low surface metal density can further impair efficiency.[8,9] To overcome these limitations, some alternative chelator complexes have been suggested, including magnetic anoparticles,[10] cobalt-based affinity resins (Talon),[11] and gels.[12] However, the efficiency of these systems have not been clearly proven to be superior to others, they are relatively expensive, and they may require longer operation times.[13]

Here, we have hypothesized that the efficiency of His-tagged protein purification could be improved by enhancing the penetration of proteins into the matrix while presenting a high density of metal ions. We developed a straightforward synthetic scheme (Scheme 1) to produce particles where the metal-chelating moiety, nitrilotriacetic acid (NTA),[14] is distributed throughout the entire matrix. The absence of a separate coating step may reduce the clogging of matrix pores during synthesis.

The NTA monomer was formed by reacting *N*,*N*-bis(carboxymethyl)-L-lysine in 0.4 M NaOH solution with acryloylchloride in toluene (upper reaction in Scheme 1). The solvent was evaporated in vacuo followed by removal of sodium ions. The oily NTA monomer was obtained by lyophilization; its identity (2,20-(5-acrylamido-1-carboxypentylazanediyl) diacetic acid) was confirmed by ^{1}H NMR (Figure S2 in the Supporting Information). 15 mol % NTA monomer was dissolved in Tris/HCl buffer along with 66 mol% acrylamide, 2.6 mol% *N*,*N*′-methylenebisacrylamide, and 16.4 mol% acrylic acid. The incorporation of acrylic acid into the microgels was done primarily to reduce aggregation and to enhance particle swelling.[15] The natural tendency of colloidal particles to aggregate is due to the thermal energy of the particles (Brownian motion) and from van der Waals interactions.[16] The incorporation of acrylic acid into the microgels increases electrostatic repulsion between particles, which reduces the tendency to aggregate.[17] In addition, the enhanced swelling due to the acrylic acids [18] reduces the effect of van der Waals forces[19] between the particles, which further reduces the tendency to aggregate. Similar concentrations of acrylic acid have been found to be successful in preventing aggregation of microgel systems in both organic and aqueous media.[20]

A water-in-oil emulsion was produced by dropwise addition of this solution to dodecane with 1% Span 80 (see also the Experimental Section). The emulsion was probe-sonicated and purged with nitrogen. Redox polymerization was initiated by adding 150 μL aqueous ammonium persulfate solution (0.1 g mL^{-1}) and 100 μL *N*,*N*,*N*′*N*′-tetramethylethylendiamine (TEMED). Particles were precipitated with methanol for 1 h, isolated by centrifugation, and suspended in concentrated 1.5 M aqueous $NiSO_4$ solution for 12 h. Lastly, the Ni^{2+} charged microgels were washed with deionized water to remove the unbound nickel ions. The resultant microgel particles were uniform in size, with an average diameter of 6.5 ± 0.8 μm (by Coulter counter).

To evaluate the ability of the microgel to reversibly and selectively bind His-tagged proteins, 0.2 mg of microgels were incubated for 20 min at room temperature in 20 μg/600

μL solutions of His-tagged GFP or untagged GFP (which have comparable molecular weights, 29 and 26.8 kDa respectively). Microgels were separated from the supernatants by centrifugation (1000 rpm, 2 min) and 600 μL of 300 mM imidazole solution was added to release the bound protein from the nickel. The binding and the recovery abilities of the microgels were determined from the emission intensities of the media (Figure 1a and b). Addition of the microgel particles followed by their removal reduced the emission intensity of the His-tagged GFP in free solution to zero, indicating a very high binding efficiency In contrast, the concentration of untagged GFP hardly changed, indicating little binding to the microgels in the absence of the histidine tag. Treatment of the His-tagged GFP loaded microgels (Figure 1c) with 300 mM imidazole solution released the protein with a recovery efficiency of approximately 65% (determined from Figures 1a and b by NIH ImageJ analysis program[21]). The same microgel particles were used for a second and third time, separated by washes with water. Protein recovery values of 79 and 77% were obtained after the second and third uses, suggesting that there may be accumulation of proteins in the particles with repeated use. However, efficiency was not affected. Incomplete desorption of proteins from IMAC systems is a well-recognized phenomenon that has been attributed to electrostatic interactions between proteins and matrices, hydrophobic interactions, and donor-acceptor (coordination) interactions of exposed amino acid residues with the metal-ions residues.[5,22] The recovery rates obtained here are high compared to those obtained with some other IMAC systems (e.g., magnetic nanoparticles),[6,12,23] possibly due to the hydrophilic structure of the microgels.[22]

To determine the ability of the microgels to purify His-tagged proteins directly from a cell lysate, 1 mg of microgels were introduced into a suspension of recombinant His-tagged ferritin lysed extracts[24] (≈20 kD, from *Escherichia coli* BL21). The suspension was agitated for 20 min at 4 °C then the microgels were separated by centrifugation (2000 rpm, 2 min). Particles were washed with deionized water to remove residual lysate and subsequently washed with 40 mM aqueous imidazole solution (wash 1 in Figure 1d) and 300 mM aqueous imidazole solution (washes 2 and 3 in Figure 1d). Proteins were collected from each step for analysis by SDS-PAGE (Figure 1d) which confirmed the purification of the desired protein. Furthermore, only trace amounts of other proteins were washed off by the 40 mM imidazole solutions suggesting mini mal non-specific interaction with proteins.

The internal structure and nickel ion density in the microgel was examined by dual-beam microscopy (a combination of a focused ion beam with an electron beam) that allows SEM imaging and local elemental analysis by energy-dispersive X-ray (EDX) of localized cross-sections (FEI Nova 200 Nanolab). The microgel particles exhibited micrometer-scale corrugated features with channels on the outer surface and pores in the body (Figure 2a). This structure is typical of microgel particles prepared by emulsion polymerization and has been attributed to a decrease in cross-link density from the center toward the periphery of the particles.[15] An EDX map for nickel of the same particle (Figure 2b) showed nickel throughout the particle. Nickel densities (Figure 2c) were approximately 20% w/w at three locations starting at the surface then progressing to the center of the microgel (marked in Figure 2a). These results confirmed that our method produced high concentrations of nickel from surface to core.

Confocal laser scanning microscopy (Figure 2d) of microgels incubated in His-tagged GFP solution (6 μg/250 μL) for 1 h showed penetration of the His-tagged protein to a depth of approximately half the radius of the particle (i.e., roughly 82.5% of the sphere volume).

The capacity of 0.5 mg of microgels to bind proteins was quantitated by incubating them in 200 μL of cell lysate, then measuring the eluted proteins with a Bradford Coomassie brilliant blue assay[25] (Figure 3). By way of comparison, the same mass of new, unused, commercially available beads (Ni-NTA Agarose, Qiagen Inc., Chatsworth, CA) bound around 3.7 times less protein. To address the potential contribution of differences in particle size between the commercial beads and microgels (58 ± 15.6 μm versus 6.5 ± 0.8, respectively), we synthesized microgel particles of equivalent size (51.1 ± 21 μm). The protein yields per unit mass of the microgels were three times higher than of the commercially available beads, indicating that regardless of size, the microgel is more efficient than conventional beads. The superior efficiency of the microgels over the commercial beads was also demonstrated for His-tag proteins of higher and of lower molecular weights (Figure S3).

Measurements of the particle specific surface area, pore volume, and average pore width were performed using the Brunauer–Emmett–Teller (BET) nitrogen adsorption method[26] with an ASAP 2020 accelerated surface area and porosimetry analyzer. The accessible surface area (Table 1) of the commercial beads was almost three times lower than of the microgel particles of the same size. The specific surface area of the smaller microgels was 26% larger than for the larger ones. The pore volumes were ten times larger in the microgels than in the commercial beads, and the pore widths were three times larger.

The enhanced performance of the microgels was potentially due to contributions of various factors. One was the relatively high Ni content in the microgels (see Figure 2C) compared to 3.2 ± 1.8% in the commercial particles ($p < 0.0002$ compared to the 6.5 and 51 μm microgels).

The higher Ni content could have been due to the proportion of acrylic acid, since acrylic acid groups confined in a 3D structure can complex with metal ions.[27] Three different batches of microgels were synthesized to assess the contribution of acrylic acid to the efficiency of these microgels: a) microgels containing 16 mol% of acrylic acid without NTA (NTA monomers were replaced with acrylamide monomers); b) microgels as in (a) with 32 mol% acrylic acid; and c) microgels composed of 100 mol% acrylic acid. These particles were loaded with nickel as described above and the nickel densities were measured by X-ray photoelectron spectroscopy. The densities of nickel were 1.06, 3.6, and 7.58% w/w for particles a, b, and c, respectively, compared to more than 20% w/w obtained with 16 mol% NTA (see above), indicating that acrylic acid does not play a major role in the metal-chelating property of these microgels. Another potential contributer to the enhanced performance was the Ni-bearing surface area available for protein binding. The microgels allowed much deeper penetration of proteins within the particles (Figure S1). Particle size could also affect the surface available, in that it determines the surface-area-to-volume ratio of the particles. In fact, the 22% higher protein binding in the smaller microgels compared to the larger microgels ($p < 0.02$ is very similar to the difference in specific surface area

between them (26%). The slightly higher protein binding by the smaller microgels was not the primary reason for the emphasis on them; they were easier to manufacture, had less tendency to aggregate, and could be easier to dispense.

We have successfully synthesized protein-binding microgels from NTAs and other monomers. They were produced by two simple synthetic steps amenable to large-scale production, which may reduce the high costs associated with many protein purification systems.[22] The versatile acrylic backbone[28] will allow easy tuning of particle properties to modify performance as desired. When loaded with Ni^{+2}, the microgels offer an efficient alternative to current methods of enriching, immobilizing and purifying proteins, and possibly other biomolecules. This new system has a high nickel density, regenerating abilities for reuse (Figure S4), superior performance in the presence of reduction agents (Figure S5), and is easily penetrated by proteins in solutions. Particle size and degree of crosslinking may also play a role in formulation performance. This approach may be applicable in other technologies involving immobilization and separation of biological molecules impurities as well as surface coating[29] and water purification.

Experimental Section

Materials and Methods

Reaction solvents were of analytical grade and were used as received from Omnisolv. Acryloylchloride, NaOH, Urea, *N*,*N*-bis(carboxymethyl)-L-lysine, acrylamide, *N*,*N*′-methylenebisacrylamide, acrylic acid, imidazole, ammonium persulfate, Tris/HCl, *N*,*N*,*N*′*N*′-tetramethylethylendiamine (TEMED), dodecane, Dowex 50WX8 and Span 80 were purchased from Sigma–Aldrich. Recombinant His-tagged Enhanced Green Fluorescent Protein (≥97% purity, Ex./Em. = 488/507 nm) was purchased from Cell Sciences (Canton, MA). Recombinant Green Fluorescent Protein (≥95% purity, Ex./Em. = 395/507 nm) was purchased from Abcam (Canton, MA). All data collected are presented as mean ± SD of at least four samples. A Student's t-test was used to compare data sets. p values < 0.05 were considered to reflect statistical significance.

The modification of *N*,*N*-bis(carboxymethyl)-L-lysine was documented by ^{1}H-NMR spectra using a Varian Mercury 500 MHz spectrometer at 25 °C in D_2O. Photoluminescent spectra were collected on Tecan Infinite M200 micro plate reader (Tecan Austria, Austria) with an excitation wavelength of 488 nm (for His-tagged green fluorescent protein) and 395 nm (for untagged green fluorescent protein). Fluorescent images of the microgel loaded with His-tagged green fluorescent protein were obtained by using fluorescence microscopy (Carl Zeiss, Inc., model HAL 100, Germany). Confocal microscopy was performed on a PerkinElmer Ultraview Spinning Disk system (PerkinElmer, USA) mounted on a Zeiss Axiovert 200m (Carl Zeiss Microimaging, Germany).

Fabrication of Microgel Particles in a Water-in-Oil Emulsion

acryloylchloride (530 μL) were dissolved in toluene (25 mL) and added dropwise to an ice-cooled NaOH solution (0.4 M) of *N*,*N*-bis(carboxymethyl)-L-lysine (1.6 g in 50 mL). The solution was allowed to stir overnight followed by the evaporation of toluene by rotary evaporation. Sodium ions were removed with Dowex 50WX8. Dowex was washed several

times with DDW until pH 7 was achieved. Then, lyophilization was carried out, which resulted in thick oil. 2,20-(5-acrylamido-1-carboxypentylazanediyl) diacetic acid (0.23 g), acrylamide (0.227 g), *N*,*N*′-methylenebisacrylamide (20 mg), acrylic acid (55 μL) and ammonium persulfate solution (0.1 g mL^{-1}, 150 μL) were dissolved in Tris/HCl (8 mL, 50 mM, pH 8.5), under nitrogen. A concentrated W/O emulsion was formed by dropwise addition of the monomers solution into a continuous oil phase (dodecane plus 1% Span 80). The emulsion was probe-sonicated (Vibra Cell sonicator, Sonics & Materials, Danbury, CT) in a 100 mL flask for 30 s (15 cycles of 2 s, with 2 s of no sonication in between) using a probe set at 40% power and purged with nitrogen to remove residual oxygen. Redox polymerization of the concentrated W/O emulsion was initiated by adding TEMED (100 μL), and the reaction was allowed to proceed for 1 h. Particles were precipitated with methanol, isolated by centrifugation (1500 rpm for 3 min) and re-suspended in $NiSO_4$ hexahydrate aqueous solution (1.5 M) for 12 h. The Ni^{2+}-charged microgel were washed and centrifuged six times to separate the microgel particles from unbound nickel ions. Microgels of larger size were fabricated by homogenizing similar monomeric solutions as mentioned above at 2000 rpm. The zeta potential in DDW for microgels with and without nickel was −20.1 ± 0.5 and −42.1 ± 1.9, respectively (ZetaPALS, Brookhaven Instruments Corp, Holtsville, NY).

Milling, Nickel Ion Density, and imaging

We used Dual Beam from FEI, model Nova Nanolab 200 (XT Nova Nanolab, Hillsboro, OR, USA). Cutting/milling technique uses a dense beam of Ga^+ ions to mill deep trenches in the area of interest. The source of the electron beam is a field emission gun with accelerating voltages of between 5 and 30 kV. SEM images of the site-specific sample have been taken using field emission SEM operating at 200 eV–30 keV.

Surface-Area Measurements

Surface-area measurements were carried out using the BET nitrogen adsorption method with an ASAP 2010 apparatus (Micromeritics, Japan), after pre-treating the samples overnight under vacuum at room temperature. For the calculation of the BET specific surface area, relative pressures in the range of 0.05–0.2 were used.

Protein Purification Procedure

Isopropyl-*β*-D-thiogalactopyranoside-induced *E. coli* bacterial cultures[30]expressing His-tagged human ferritin were pelleted and frozen at −80 overnight. The cells were lysed using a 1X concentration of Sigma Cellytic B Cell Lysis reagent, 100 μL of 100 mg mL^{-1} lysozyme, and ≈250 units of Sigma Benzonase nuclease. The lysis solution was spun at 16 000 rpm for 20 min, resuspended in 20 mM Tris (Base), 6 M Urea, and spun again at 16 000 rpm for 20 min. The lysate protein solution was exposed to the particulate affinity matrices for about 20 min, centrifuged (1000 rpm, 2 min), and washed with 20 mM Tris, 20 mM NaCl, pH 8.1, and with 50 mM Tris pH 8.1, 50 mM NaCl, 40 mM imidazole solution. The histidine-tagged protein solution was eluted from each matrix using 50 mM Tris pH 8.1, 50 mM NaCl, and 300 mM imidazole solution.

Supplementary Material

Refer to Web version on PubMed Central for supplementary material.

References

1. Smith C. Nat Meth. 2005; 2:71.
2. Terpe K. Appl Microbiol Biotechnol. 2003; 60:523. [PubMed: 12536251]
3. Braun P, Hu Y, Shen B, Halleck A, Koundinya M, Harlow E, LaBaer J. Proc Natl Acad Sci USA. 2002; 99:2654. [PubMed: 11880620]
4. Kim JS, Valencia CA, Liu R, Lin W. Bioconjug Chem. 2007; 18:333. [PubMed: 17311440]
5. Gutierrez R, d Valle EMM, Galn MA. Sep Purif Rev. 2007; 36:71.
6. Lee IS, Lee N, Park J, Kim BH, Yi YW, Kim T, Kim TK, Lee IH, Paik SR, Hyeon T. J Am Chem Soc. 2006; 128:10658. [PubMed: 16910642]
7. Xu C, Xu K, Gu H, Zhong X, Guo Z, Zheng R, Zhang X, Xu B. J Am Chem Soc. 2004; 126:3392. [PubMed: 15025444]
8. Johnson RD, Arnold FH. Biotechnol Bioeng. 1995; 48:437. [PubMed: 18623507]
9. Liesiene J, Racaityte K, Morkeviciene M, Valancius P, Bumelis V. J Chromatogr A. 1997; 764:27. [PubMed: 9098994]
10. Franzreb M, Siemann-Herzberg M, Hobley TJ, Thomas OR. Appl Microbiol Biotechnol. 2006; 70:505. [PubMed: 16496138]
11. Bohren KM, Gabbay KH, Owerbach D. Protein Expr Purif. 2007; 54:289. [PubMed: 17459725]
12. Ha EJ, Kim YJ, An SS, Kim YR, Lee JO, Lee SG, Paik HJ. J Chromatogr, B: Analyt Technol Biomed Life Sci. 2008; 876:8.
13. Ausubel, FMB.; Brent, R.; Kingston, RE.; Moore, DD.; Seidman, JG.; Smith, JA.; Struhl, K.; Albright, LM.; Coen, DM.; Varki, A., editors. Current Protocols in Molecular Biology. Wiley; New York: 2003.
14. Ko YG, Kang YS, Park H, Seol W, Kim J, Kim T, Park HS, Choi EJ, Kim S. J Biol Chem. 2001; 276:39103. [PubMed: 11495919]
15. Saunders BR, Vincent B. Adv Colloid Interface Sci. 1999; 80:1.
16. Tielemans M, Roose P, Groote PD, Vanovervelt JC. Prog Org Coat. 2006; 55:128.
17. Kratz K, Hellweg T, Eimer W. Colloids Surf A. 2000; 170:137.
18. Saunders BR, Crowther HM, Vincent B. Macromolecules. 1997; 30:482.
19. López-León T, Ortega-Vinuesa JL, Bastos-González D, Elaïssari A. J Phys Chem B. 2006; 110:4629. [PubMed: 16526694]
20. Lawrence DB, Cai T, Hu Z, Marquez M, Dinsmore AD. Langmuir. 2007; 23:395. [PubMed: 17209584]
21. Rasband, W.; US. National Institutes of Health. [accessed, July 2011] ImageJ. http://rsb.info.nih.gov/ij/
22. Suen SY, Liu YC, Chang CS. J Chromatogr, B: Analyt Technol Biomed Life Sci. 2003; 797:305.
23. Lee J, Xu Y, Chen Y, Sprung R, Kim SC, Xie S, Zhao Y. Mol Cell Proteomics. 2007; 6:669. [PubMed: 17208939]
24. Dong X, Tang B, Li J, Xu Q, Fang S, Hua Z. J Microbiol Biotechnol. 2008; 18:299. [PubMed: 18309275]
25. Bradford MM. Anal Biochem. 1976; 72:248. [PubMed: 942051]
26. Brunauer S, Emmett PH, Teller E. J Am Chem Soc. 1938; 60:309.
27. Zeng QB, Ye QZ, Xu JR, Fu RW. Chin Chem Lett. 2002; 13:436.
28. Vinogradov SV. Curr Pharm Des. 2006; 12:4703. [PubMed: 17168773]
29. Scott EA, Nichols MD, Cordova LH, George BJ, Jun YS, Elbert DL. Biomaterials. 2008; 29:4481. [PubMed: 18771802]
30. Schwartz SH, Qin X, Zeevaart JA. J Biol Chem. 2001; 276:25208. [PubMed: 11316814]

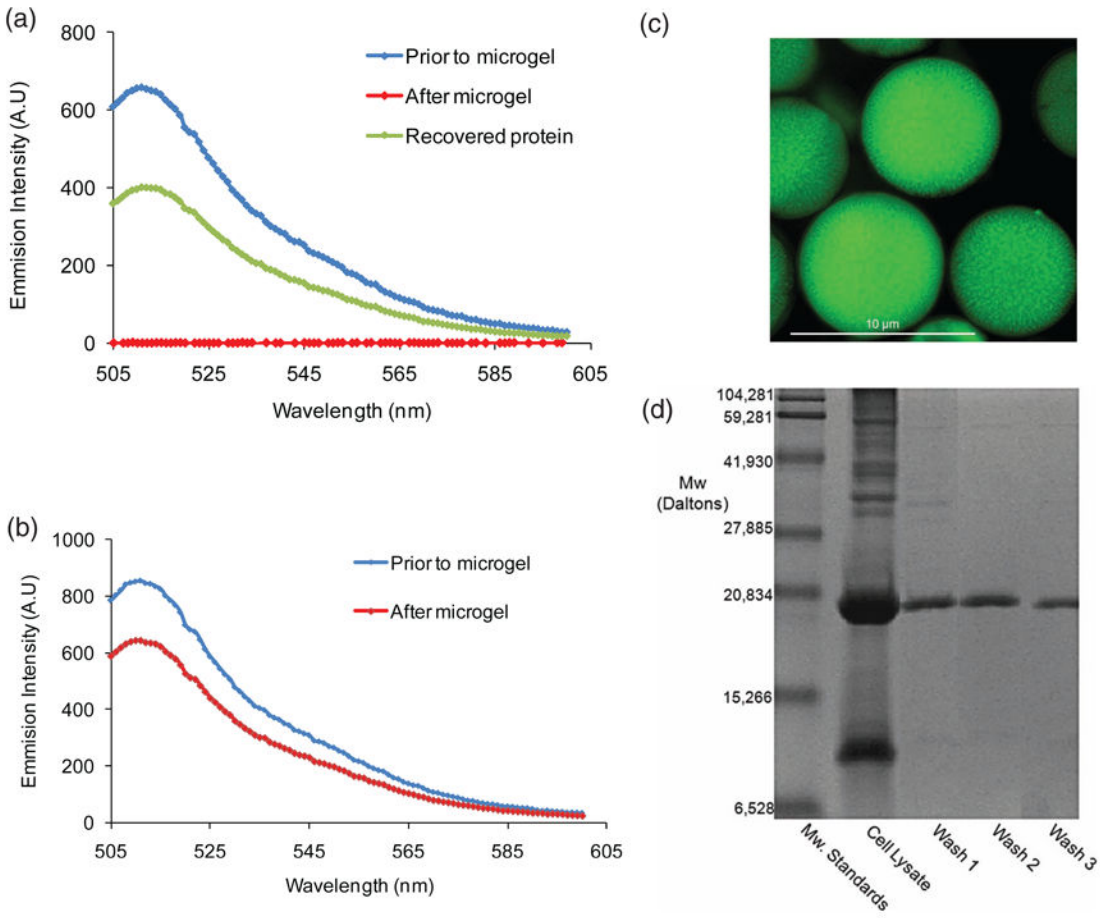

Figure 1.

a) Emission intensities of the fluorescence spectra of His-tag GFP free in solution before (upper curve) and after (lower curve) binding with microgels. The middle curve represents the protein recovered after application of 300 mM imidazole solution. b) Fluorescence spectra of the emission intensities of untagged GFP in the solutions before (upper curve) and after (lower curve) microgel introduction. c) Fluorescent image of microgel particles loaded with His-tag GFP. d) SDS-PAGE of His-tag ferritin isolated from cell lysates with microgels. From left to right: molecular weight standards, cell lysates, proteins washed from microgels with 40 mM imidazole solution (wash 1), and twice with 300 mM imidazole solution (washes 2 and 3).

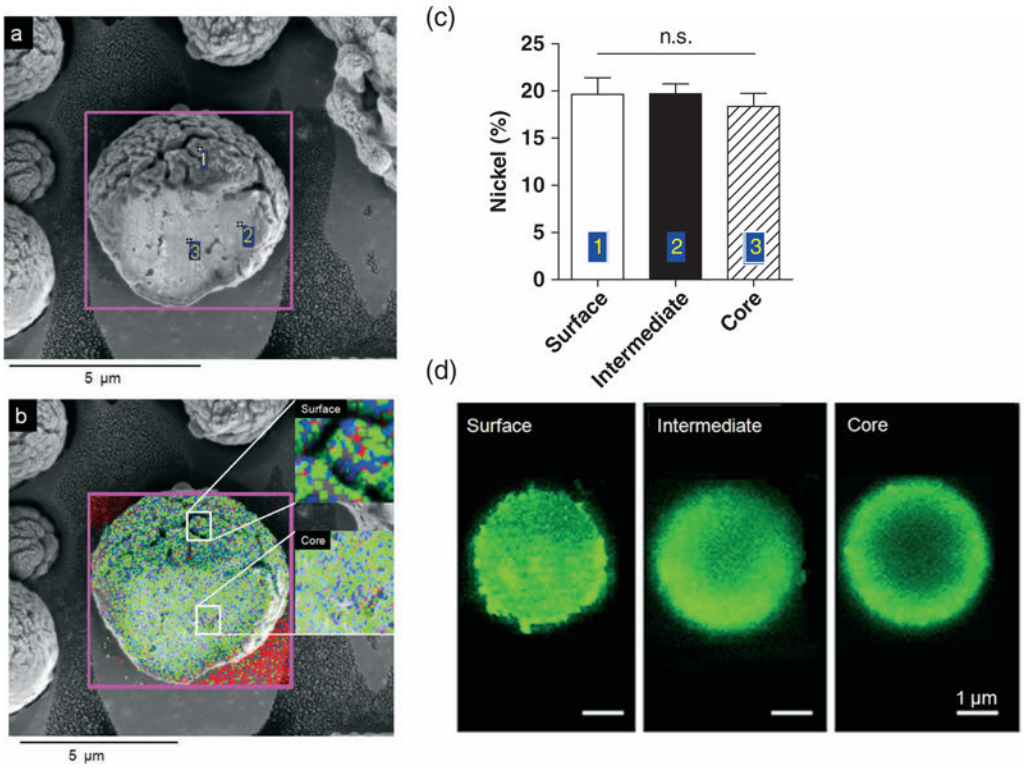

Figure 2.

a) SEM microscopy image of ion-milled microgel particle displaying the surface and the core. Numbers indicate locations analyzed for nickel content at (1) the surface, (2) an intermediate location, and (3) the core. b) SEM/EDX map for nickel in the same particle shown in (a). Nickel is indicated by turquoise dots. Insets: enlargement of the surface and the core. Pores are in black. c) Nickel mean density (% w/w) throughout the microgel particle at the locations indicated in (A). Data are given as the mean value ± standard deviation (SD) (n = 8); n.s. = no statistically significant difference by ANOVA. d) Fluorescent confocal microscopy images of a microgel incubated in His-tagged GFP solution, showing the surface and cross sections at depths of 1.5 µm (intermediate) and 3 µm (core). The excitation wavelength was 488 nm.

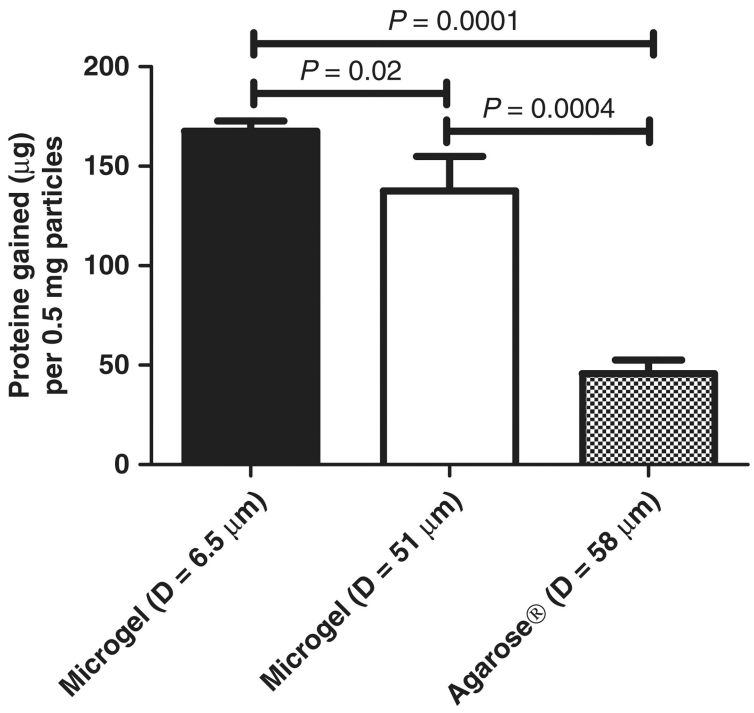

Figure 3.

Efficiency of microgels of different sizes and of commercially available beads in purifying His-tagged ferritin from cell lysate. Data are mean ± SD, (n = 8).

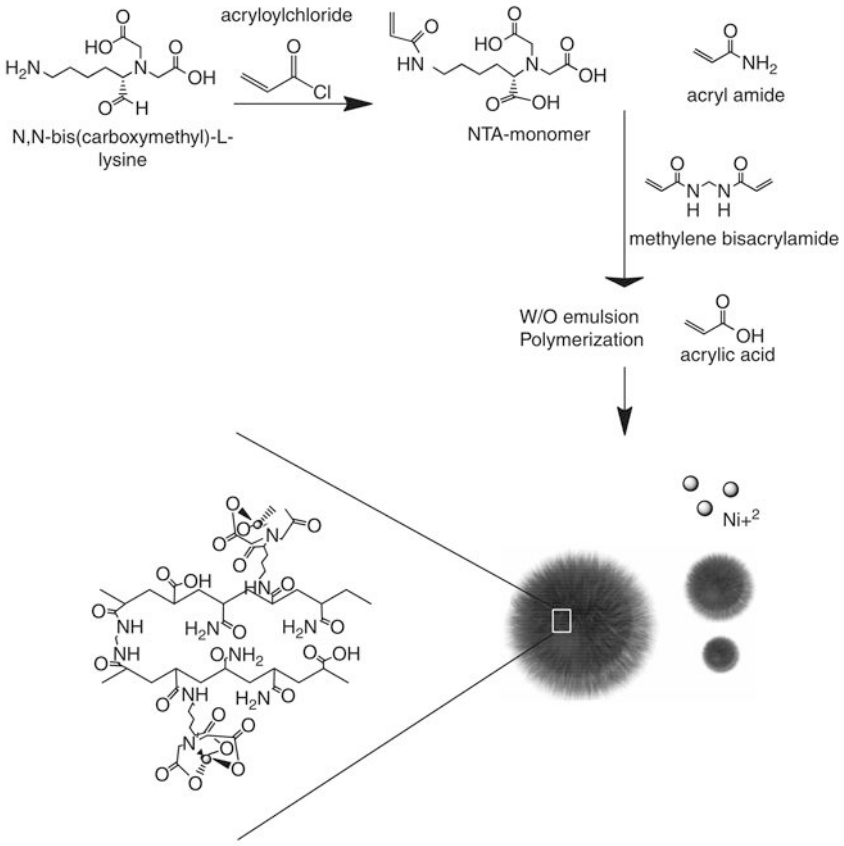

Scheme 1.

Synthesis of the NTA monomer and fabrication of NTA/Ni^{+2} microgel particles. The NTA monomer is 2,20-(5-acrylamido-1-carboxypentylazanediyl) diacetic acid.

Table 1

Surface characteristics of microgels and commercial beads. All data are shown as mean ± SD.

Sample	Average size [μm]	Surface area [m^2 g^{-1}]	Pore volume [cm^3 g^{-1}]	Average pore width [nm]
Microgel	6.5 ± 0.8	12.95 ± 0.04	0.0286	8.83
Microgel	51.1 ± 21	10.28 ± 1.28	0.0301	9.98
Commercial[a)]	58 ± 15.6	3.52 ± 0.29	0.0029	3.27

a)Ni-NTA Agarose, Qiagen Inc., Chatsworth, CA.